

International Journal of Modern Physics B
 © World Scientific Publishing Company

RANGE-DEPENDENT DISORDER EFFECTS ON THE PLATEAU-WIDTHS CALCULATED WITHIN THE SCREENING THEORY OF THE IQHE

AFIF SIDDIKI

*Physics Department, Arnold Sommerfeld Center of Theoretical Physics, and CeNS,
 Ludwigs-Maximilians-Universität München,
 Theresienstr. 37, D-80333 München, Germany
 siddiki@theorie.physik.uni-muenchen.de*

ROLF R GERHARDTS

*Max-Planck-Institut für Festkörperforschung,
 Heisenbergstr. 1 D-70569 Stuttgart, Germany
 R.Gerhardts@fkf.mpg.de*

Received 25 August 2006

We summarize the screening theory of the integer quantized Hall effect (IQHE) and emphasize its two key mechanisms: first, the existence, in certain magnetic field intervals, of incompressible strips, with integer values of the local filling factor and quantized values of longitudinal and Hall resistivity, and second, the confinement of an imposed dissipative current to these strips, leading to the quantization of the global resistances. We demonstrate that, without any localization assumption, this theory explains the enormous experimental reproducibility of the quantized resistance values, as well as experimental results on the potential distribution in narrow Hall bars. We further demonstrate that inclusion of long-range potential fluctuations allows to apply the theory to wider Hall bars, and can lead to a broadening of the quantum Hall plateaus, whereas short-range disorder tends to narrow the plateaus.

Keywords: Integer quantized Hall effect; incompressible strips; long-range disorder.

1. Introduction

Twenty-five years after its discovery, one should believe that the integer quantized Hall effect (IQHE),¹ observed on two-dimensional electron systems (2DES) in high magnetic fields, is well understood. Indeed it is often “explained” as a consequence of Landau quantization and localization of electronic states, within a single particle picture that considers the Coulomb interaction between the electrons as irrelevant. This “explanation” ignores, however, important aspects of the IQHE, e.g. the enormous accuracy with which the quantized resistance values can be reproduced experimentally.² It also can not describe, or even contradicts, recent experiments by E. Ahlswede *et al.*³ on the Hall potential distribution in narrow Hall bars (width $\lesssim 20 \mu\text{m}$). A major purpose of the present paper is to emphasize that both, these

recent experiments and the enormous experimental reproducibility of the quantized resistance values, can be understood within a conventional local transport theory, which takes into account the peculiar screening, i.e. Coulomb interaction, effects in 2DES under high magnetic fields, but avoids any localization assumptions. Since some details of this theory have already been published,^{4,5} we focus here on the key mechanisms of this approach. Moreover, we add a discussion of long-range potential fluctuations, which become important in wider Hall bars and indicate a possible extension of our approach. The systems we have in mind contain a 2DES in a GaAs/(AlGa)As heterostructure, populated by ionized (Si-)donors, which are distributed randomly in a plane parallel to that of the 2DES.

2. Importance of screening induced edge profile for the IQHE

2.1. Bulk resistivity and accuracy of the IQHE

If we admit that a bulk theory for the resistivity of a homogeneous system, like that of localization,⁶ yields quantization in a regime of filling factors, say around $\nu = 2$, the edge regions of a finite sample, where the filling factor drops to zero, must lead to errors. If we estimate the error by the ratio of (width of edge region) over (sample width), a typical depletion length of about 100 nm and an accuracy of 10^{-8} or better requires a sample width of ten meters or more. Thus, a theory for homogeneous samples cannot explain the accuracy of the IQHE in samples of realistic size.

2.2. Edge states and screening

The sample edges are taken into account in the Büttiker picture, which considers an upwards bending of the Landau energy levels as a consequence of the confining potential.⁷ The relevant, current-carrying edge states are believed to be the states of the Landau bands immediately at the Fermi edge. This picture traces the IQHE back to the conductance quantization in quasi-1D systems. However, in the quasi-1D situation all channels (Landau bands) carry the same amount of current, which seems not to be true in the Ahlswede experiment.³

This edge-state picture has been criticized theoretically by Chklovskii *et al.*⁸ who argue that, for a smooth confinement potential, it leads to a step-like density profile, with plateaus corresponding to integer filling factors. To change the smooth density profile at vanishing magnetic field, $B = 0$, into this B -dependent step-profile would cost a lot of Coulomb energy. *Screening* will avoid such large and energetically expensive changes of the density profile. *Compressible strips* with nearly perfect screening will occur, in which a partially filled Landau level (LL) is pinned to the Fermi energy, so that at zero temperature the total potential within the strip is flat, while the density varies very similar to the $B = 0$ case. Adjacent compressible strips will be separated by *incompressible strips* (ISs). There the Fermi level is between neighboring LLs, the density is constant, and the potential varies by the amount of a cyclotron energy across the IS. We assume here and in the following spin degeneracy.

Some questions remain, which we have to answer: Do all these ISs really exist? Where does the current flow ?

2.3. The Ahlswede experiment on the Hall potential distribution

Important answers were given by the experiments of Ahlswede and coworkers,^{3,9,10,11} who used a scanning force microscope to measure the local electrostatic force across a narrow Hall bar. From this they calculated the Hall potential, which determines the local current distribution. They observed the quantized Hall effect (near filling factors $\nu = 2$ and $\nu = 4$) and, related to this, three different types of potential drop across the Hall bar:³ (I), a linear drop for B -fields well outside a QH plateau; (II), a non-linear drop in the center region, for B -fields near the upper edge of a QH plateau. (III), for B -fields well within a plateau a potential profile was observed which is constant in the center and drops across strips, which move with decreasing B towards the edges of the Hall bar. In all cases *only one current carrying strip* at each edge is observed, at the position expected for the innermost *incompressible strip*!

Earlier calculations,^{12,13} which describe an imposed *dissipationless* Hall current along a Hall bar, can not explain these different types of potential drop. Apparently we need a *local transport theory* that is able to describe *dissipative currents* in the presence of compressible and *incompressible strips*.

3. Screening theory of the IQHE

3.1. Local distribution of dissipative currents in the IQH regime

We consider a simplified Hall bar in the stripe $|x| \leq d$ of the x - y -plane, and assume translation invariance in y -direction. We impose a fixed total current $I_0 = \int_{-d}^d dx j_y(x, y)$ along the Hall bar and write for the current density \mathbf{j} Ohm's law with a local resistivity tensor $\hat{\rho}$ and a driving electric field \mathbf{E} , which we assume to be the gradient of the position-dependent electrochemical potential μ^* ,

$$\hat{\rho}(\mathbf{r})\mathbf{j}(\mathbf{r}) = \mathbf{E}(\mathbf{r}) \equiv \nabla\mu^*(\mathbf{r})/e, \quad \hat{\rho}(\mathbf{r}) = [\hat{\sigma}(n_{\text{el}}(\mathbf{r}))]^{-1}. \quad (1)$$

The resistivity tensor, with components $\rho_{yy} = \rho_{xx} = \rho_l$ and $\rho_{xy} = -\rho_{yx} = \rho_H$, and its inverse, the conductivity tensor $\hat{\sigma}$, are assumed to depend only on the local electron density $n_{\text{el}}(x)$. The dissipative current density vanishes in thermodynamic equilibrium, since then μ^* is constant over the sample.

In the stationary, translation-invariant case, one has $\nabla \cdot \mathbf{j}(\mathbf{r}) = 0$ and $\nabla \times \mathbf{E}(\mathbf{r}) = \mathbf{0}$, and, with $\partial_y j_y = 0$ and $\partial_y E_x = 0$, one sees $\partial_x j_x = 0$ and $\partial_x E_y = 0$, so that $j_x(x) \equiv 0$ and $E_y(x) = E_y^0$ independent of x . With this and Eq. (1) one immediately obtains the components of current density and driving electric field,

$$E_y(x) \equiv E_y^0, \quad j_y(x) = \frac{1}{\rho_l(x)} E_y^0, \quad E_x(x) = \frac{\rho_H(x)}{\rho_l(x)} E_y^0, \quad (2)$$

in terms of the resistivity components. Knowing the field components, it is easy to calculate the position dependence of the electrochemical potential,

$$\mu^*(x, y) = \mu_0^* + eE_y^0 \left\{ y + \int_0^x dx' \frac{\rho_H(x')}{\rho_l(x')} \right\}. \quad (3)$$

If a model for the local conductivity tensor $\hat{\sigma}(n_{\text{el}}(x))$ is given, it is straightforward to calculate current distribution and electrochemical potential. For instance in the Drude model there exists no longitudinal magnetoresistance, i.e. $\rho_l(x) = m/[e^2\tau n_{\text{el}}(x)]$ is independent of B , and $\rho_H(x) = \omega_c\tau\rho_l(x)$. Thus, $j_y(x)$ is proportional to the electron density $n_{\text{el}}(x)$ and the Hall field $E_x(x)$ is independent of x , i.e. the potential varies linearly across the sample (*type I* behavior).

3.2. Current confinement to incompressible strips

As a consequence of Landau quantization, a (spin-degenerate) 2DES at (even) integer filling factor $\nu = n$ is, in the limit of vanishing temperature ($T \rightarrow 0$), inert in the sense that no elastic scattering is possible (since occupied and unoccupied electron states are separated by the cyclotron energy $\hbar\omega_c \gg k_B T$). In the absence of scattering, the resistivity components take on the free-electron values, $\rho_l(\nu \rightarrow n) \rightarrow 0$, $\rho_H(\nu \rightarrow n) \rightarrow h/(n \cdot e^2)$. The essence of our local approach is the assumption that this remains valid on (sufficiently wide) incompressible strips with integer *local* filling factor,

$$\nu(x) = n : \quad \rho_l(x) \rightarrow 0, \quad \rho_H(x) \rightarrow h/(n \cdot e^2) \quad \text{for } T \rightarrow 0. \quad (4)$$

If such ISs exist, the integral $\int_{-d}^d dx [1/\rho_l(x)] \rightarrow \infty$ diverges for $T \rightarrow 0$. Since the total imposed current $I_0 = \int_{-d}^d dx [E_y^0/\rho_l(x)]$ is fixed, this implies $E_y^0 \rightarrow 0$, and the current density tends to zero outside the incompressible strips, where $\rho_l(x)$ remains non-zero. From Eq. (2) we see also that the Hall field $E_x(x)$ vanishes outside the ISs, so that the Hall potential drops only across these strips, i.e. shows the *type III* behavior observed in the Ahlswede experiment.

If only incompressible strips with the same integer value n of the local filling factor exist, the Hall resistivity takes on the same value $h/(n \cdot e^2)$ wherever the Hall field remains finite, and can be taken out of the integral, $V_H = \int_{-d}^d dx E_x(x) \rightarrow [h/(n \cdot e^2)]I_0$. As a result, the global resistances are quantized:

$$R_l \propto E_y^0 \rightarrow 0, \quad R_H \rightarrow h/(n \cdot e^2). \quad (5)$$

The resistances are quantized, since all the current flows in the ISs. Then dissipation and entropy production vanish, i.e. assume their minimum possible values, in accordance with the rules of irreversible thermodynamics. The deviation from the quantized values becomes *exponentially small* with decreasing temperature $[\sim \exp(-\hbar\omega_c/2k_B T)]$, as a consequence of Landau quantization and Fermi statistics, without any localization assumptions.

3.3. Application to the Ahlswede experiment

To apply this formalism to the experimental situation, we have to choose a model for the conductivity tensor as function of the filling factor. We have considered two models which yield very similar results, first, an approach based on a Gaussian approximation of the collision-broadened Landau levels,^{14,15} and, second, the self-consistent Born approximation (SCBA) to the electron-impurity problem.^{4,16,17} The latter allows for a fully consistent treatment of Landau level broadening and magneto-conductivity tensor.

To obtain a position-dependent conductivity tensor, we replaced in these models the filling factor by the local filling factor of the simplified Hall bar, calculated under due consideration of screening effects. For given density profile $n_{\text{el}}(x)$ of the 2DES, we had to solve Poisson's equation under reasonable electrostatic boundary conditions. We adopted a model used by Chklovskii *et al.*,^{8,18} which assumes all charges and gates in a single plane and takes advantage of the methods of complex analysis. However, whereas these authors calculate $n_{\text{el}}(x)$ in the “electrostatic approximation” from the crude assumption of perfect screening in the 2DES, we used a self-consistent Thomas-Fermi-Poisson approximation^{19,13} (TFPA), which describes the properties of the 2DES more realistically by its density of states (DOS). To calculate $n_{\text{el}}(x)$ in Thomas-Fermi approximation, can be justified from a more reliable Hartree-type calculation, if the potential $V(x)$ confining the electrons to the Hall bar is so smooth that it is nearly constant over the extent of occupied energy eigenfunctions. If this condition is not satisfied, the TFPA may yield incompressible strips, which do not exist if the finite extent of the wavefunctions is taken into account. We found, in agreement with earlier work by Suzuki and Ando,^{20,21} that Hartree-type calculations are considerably more restrictive in predicting ISs than the TFPA. For more details see Fig.1 of Refs.4 and 5, and the related discussions.

Our Hartree-type calculations show that, for the sample widths and electron densities of interest, incompressible strips exist only in magnetic field intervals of finite width (the plateau regions of the IQHE), and that in these intervals only a single IS exists on each side of the sample, with the same integer value of the filling factor on both sides. This is in agreement with the Ahlswede experiment.

For a direct comparison with the experiment, we should realize that the scanning force microscope measures the (gradient of the) *electrostatic* potential $V(x)$, not the *electrochemical* potential $\mu^*(x)$, which we can easily calculate for given $\hat{\sigma}(n_{\text{el}}(x))$. To calculate the feedback of the imposed dissipative current on the density profile and the electrostatic potential, we assume *local equilibrium* in the stationary dissipative state, i.e. we repeat the equilibrium calculation for the position-dependent electrochemical potential and iterate the procedure with the new density profile until convergence for density profile, electrostatic and electrochemical potential is obtained. For a high imposed current I_0 , this yields a considerable change of $n_{\text{el}}(x)$.¹⁴ For a weak I_0 , however, the density change is small and the current-induced change of $V(x)$ has practically the same position dependence as $\mu^*(x)$. Therefore, in the

linear response regime it is sufficient to calculate $\mu^*(x)$ from the equilibrium density profile and to compare its position dependence with the measured change of $V(x)$.

3.4. *Simulation of non-local corrections*

Our local transport model in connection with the TFPA leads to two types of problems. We have already discussed the effect of the finite extent of wavefunctions, which prohibits ISs in edge regions, where density profile and confinement potential are too steep. As a second failure, the local relation between the statistically defined quantities like current density, resistivity tensor and gradient of the electrochemical potential will break down on scales comparable with the average distance between electrons. It also leads to artifacts like a singular current density at positions where the local filling factor assumes integer values, even if there no IS of finite width exists. We can get rid of both problems in a very simple way. We calculate the density profile $n_{\text{el}}(x)$ within the TFPA, with this the conductivity tensor $\hat{\sigma}(\nu(x)) \equiv \hat{\sigma}(x)$, and then simulate non-local effects by coarse-graining the conductivity tensor according to

$$\hat{\sigma}(x) = \frac{1}{2\lambda} \int_{-\lambda}^{\lambda} d\xi \hat{\sigma}(x + \xi), \quad \text{with } \lambda \sim \lambda_F/2, \quad (6)$$

where λ_F is the Fermi wavelength. With the coarse-grained $\hat{\sigma}(x)$, we calculate current distribution and $\mu^*(x)$.

3.5. *Summary of results*

Having emphasized the basic ingredients and the key mechanisms of our approach to the understanding of the IQHE in narrow Hall bars, we now summarize the basic results.^{4,5} For narrow GaAs Hall bars (width $\lesssim 15 \mu\text{m}$) containing a (spin-degenerate) 2DES of typical density [$n_{\text{el}}(0) \lesssim 4 \cdot 10^{11} \text{ cm}^{-2}$] we find non-overlapping magnetic field intervals of finite width, in which incompressible strips with a well defined (even) integer value of the local filling factor exist. For B values in these intervals, the imposed dissipative current is, with decreasing temperature, increasingly confined to these incompressible strips, so that the global longitudinal and Hall resistances approach the local resistivity values on these ISs. The deviation of the Hall resistance from the quantized values decreases exponentially with decreasing temperature. The intervals under discussion are thus the plateau regimes of the IQHE.

For the simple, translation invariant Hall bars, which we have considered so far, the electron density (at $B = 0$) decreases monotonously from the center towards the edges. As B decreases from high values, ISs occur first in the center, broaden rapidly, and then split into two strips at a lower B value. With further decreasing B , the strips move towards the edges, shrink, and finally disappear at a B value considerably higher than the one at which the IS with the next higher integer filling factor occurs in the center.

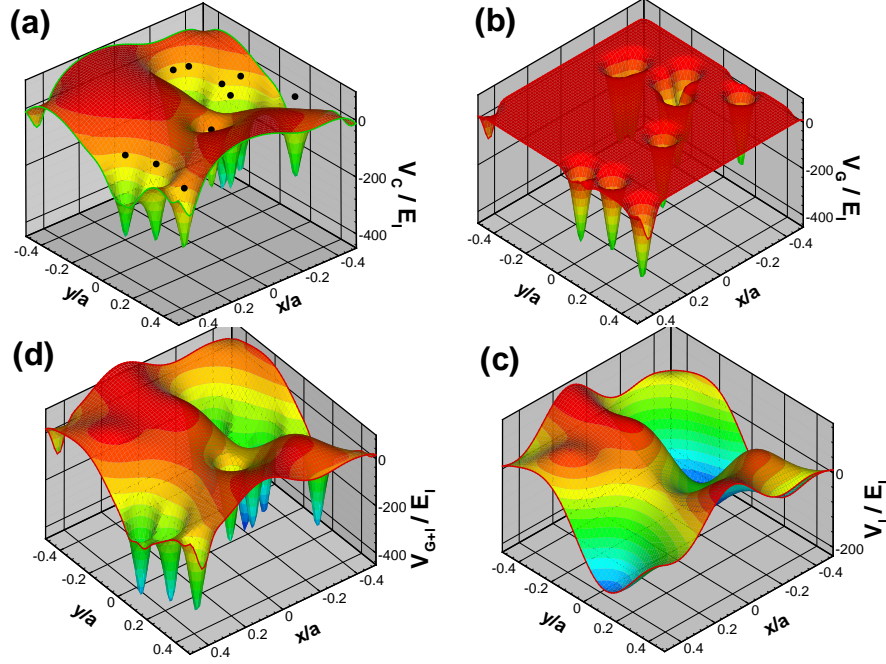


Fig. 1. Potential of $N_I = 10$ randomly distributed donors (black dots) in the unit cell of a square lattice with lattice constant $a = 3 \mu\text{m}$, at distance $z = 90 \text{ nm}$ from the 2DES, $\bar{\kappa} = 12.4$. (a) Coulomb potentials; (b) Gaussian approximation; (c) long-range part given by Fourier coefficients with $\mathbf{q} = 2\pi(n_x, n_y)/a$ for $|n_x| \leq 2$ and $|n_y| \leq 2$; (d) sum of (b) and (c). Average potentials are subtracted in (a) - (d), energy unit $E_I = \pi\hbar^2 \cdot N_I/(ma^2)$.

The widths of the ISs, and as a consequence the widths of the quantum Hall plateaus, shrink with increasing temperature,¹⁹ with increasing value of the phenomenological coarse-graining parameter λ ($\sim 20\text{-}50 \text{ nm}$), which we use to simulate non-local effects, finite width of wavefunctions, etc., and with increasing collision broadening of the Landau levels.⁴ For reasonable parameter values, the calculated position-dependence of the Hall potential shows all the different types of profiles observed in the Ahlswede experiment.

4. Long-range potential fluctuations

4.1. Separation of short- and long-range potential fluctuations

So far we have considered impurity scattering, within the SCBA, in the calculation of conductivities and level broadening of the Landau DOS. In principle we should consider randomly distributed Coulomb scatterers at a distance z from the 2DEG. However, since the SCBA does not describe coherent multi-center scattering, the overlapping long-range parts of the Coulomb potentials would lead to unphysically large damping effects. As usual we have, therefore, taken into account only the short-

range parts of the potentials, approximated by Gaussians, i.e. we have replaced

$$V_{\text{imp}}(\mathbf{r}; z) = \sum_j \frac{-e^2/\bar{\kappa}}{\sqrt{(\mathbf{r}-\mathbf{r}_j)^2 + z^2}} \quad \text{by} \quad V_{\text{Gauss}}(\mathbf{r}; z) = \sum_j \frac{-e^2}{\bar{\kappa}|z|} \exp\left(-\frac{(\mathbf{r}-\mathbf{r}_j)^2}{2z^2}\right), \quad (7)$$

where \mathbf{r} and \mathbf{r}_j are vectors within the x - y -plane. To get a feeling for the short- and long-range parts of the potential fluctuations, we have plotted in the upper left panel of Fig. 1 the potential created by ten donors distributed randomly in a square. To the right, we show the superposition of the corresponding Gaussians, i.e., the short-range part (SRP). Below we plot the long-range part (LRP), defined by the lowest order Fourier coefficients. In the lower left panel we show the sum of long-range and short-range parts, which looks qualitatively very similar to the original superposition of Coulomb potentials.

The SRP and the LRP of the fluctuating donor potential do not only look very different, they also behave very differently concerning both their dependence on the distance z between donor layer and 2DES and on the screening by the 2DES. The SRP is dominated by large Fourier coefficients and therefore decreases rapidly (exponentially) with increasing z , however is only weakly screened. The LRP, on the other hand, is dominated by low-order Fourier coefficients, thus decreases only slowly with increasing z , but is strongly screened by the 2DES. We take this as justification to treat SRP and LRP very differently. For the SRP we neglect screening effects, use the Gaussian approximation and consider it within the SCBA for the calculation of conductivities and level broadening, as we did before. To take the LRP into account, we add it to the external confinement potential and treat it together with this in the self-consistent screening calculations.

4.2. *Effect on the plateau width of the IQHE*

In Fig. 2 we simulate long-range disorder by a simple harmonic modulation potential of the same period in a narrow and a five times wider Hall bar. Without the modulation, the density profile is flatter (i.e. screening is more effective) in the wider sample, so that the Fermi energy $E_F = \bar{n}_{\text{el}}/D_0$, which yields the average filling factor $\bar{\nu} = 2$ at $\hbar\omega_c/E_F = 1$, is only slightly smaller than the energy $E_F^0 = n_{\text{el}}(x=d, B=0, T=0)/D_0$, which determines the high-magnetic-field edge of the $\nu = 2$ quantum Hall plateau (QHP) at $\hbar\omega_c/E_F^0 = 1$.

For the narrow sample, the modulation potential has little effect. It slightly enhances the confinement potential, thus increases the electron density in the center ($x = d$), and shifts the high- B edge of the QHP to slightly higher B -values. For the wider sample and sufficiently large modulation amplitude, at certain B -values additional incompressible strips may occur inside the sample. Thus, increasing amplitude of long-range disorder may lead to a broadening and stabilizing of quantum Hall plateaus, as opposed to an increase of short-range disorder, which leads to an increase of the Landau level width, i.e. a decrease of the Landau gaps and, thereby, to a shrinking of the plateaus. These different effects of short- and long-range disorder are demonstrated in Fig. 3 and Fig. 4, respectively. Figure 3 is calculated for

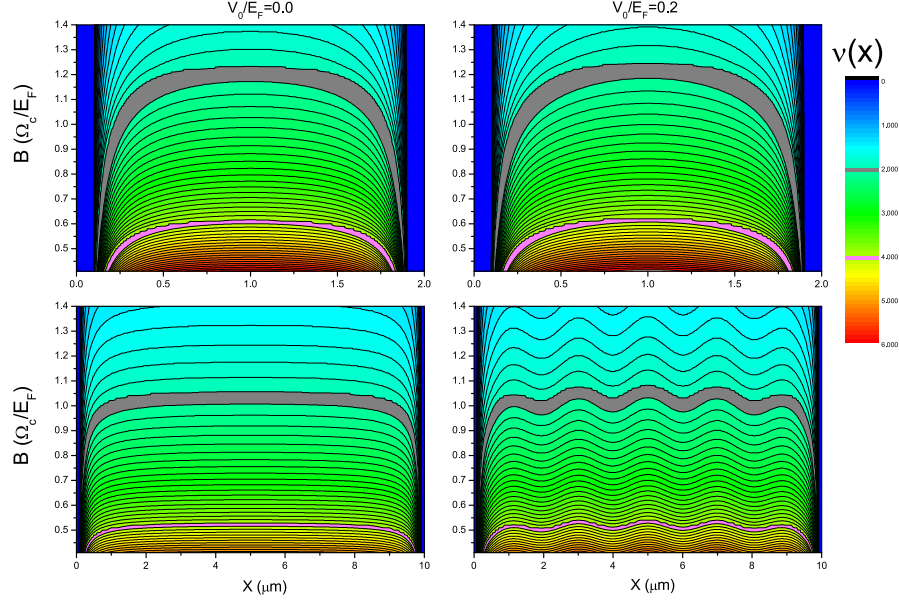


Fig. 2. Color-coded plot of the local filling factor versus position x and cyclotron energy $\Omega_c = \hbar\omega_c$ without (left panels) and with (right panels) external modulation potential $V_{\text{mod}}(x) = -V_0 \sin(p\pi x/2d)$ in $0 \leq x \leq 2d$, for $2d = 2 \mu\text{m}$ and $p = 1$ (upper) and $2d = 10 \mu\text{m}$ and $p = 9$ (lower panels); gray indicates $\nu(x) = 2$ and pink $\nu(x) = 4$. Average densities: $2.88 \cdot 10^{11} \text{ cm}^{-2}$ (upper) and $3.69 \cdot 10^{11} \text{ cm}^{-2}$ (lower panel); $k_B T/E_F = 0.02$, $V_0/E_F = 0.2$; at $T = 0$, $B = 0$, in all cases the width of the symmetric density profile is $2d = 200 \text{ nm}$.

Gaussian potentials, like in Eq. (7), with a range $R = \sqrt{2}z$, and γ_I is proportional to the density and the square of the potential amplitude of the impurities.

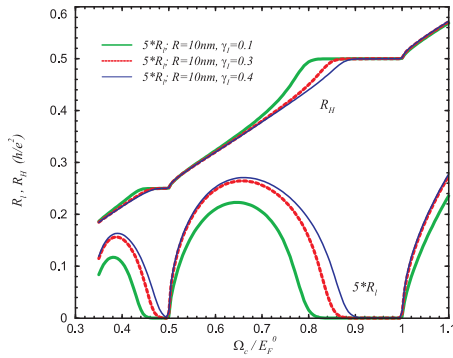


Fig. 3. Dependence of the resistance curves on the strength γ_I of short-range disorder. For details see Ref. 4.

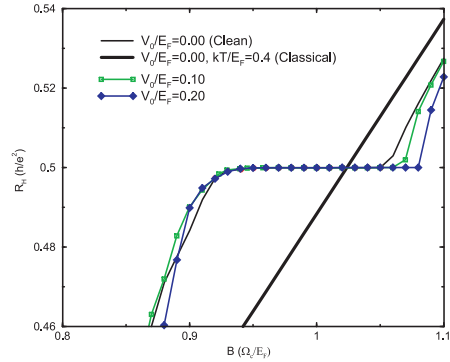


Fig. 4. Dependence of the $\nu=2$ Hall plateau on the amplitude V_0 of long-range disorder for the sample of width $2d = 10 \mu\text{m}$ of Fig. 2.

5. Conclusion

Long-range potential fluctuations across wide Hall bars may produce additional incompressible strips, and thereby stabilize the quantum Hall plateaus, shift them to higher B fields, and broaden them. Thus, the screening theory of the IQHE, which explains the experimental results on narrow Hall bars very well, has also potential for application to wide samples. Although this theory in its present state contains a number of phenomenological assumptions, which in the future may be justified or abandoned, we believe that it contains the clue for the understanding of the IQHE and its astonishing reproducibility even in narrow samples: In the plateau regime of the IQHE the current is forced to flow through channels in the sample, where the quantization conditions hold locally. Screening is a mechanism to provide, in inhomogeneous systems and in magnetic field intervals of finite width, such channels in the form of incompressible stripes or, more generally, percolating incompressible regions. Localization effects may play a role in macroscopic samples, but they seem not to be relevant in the narrow samples considered here.

Acknowledgements

We are grateful to E. Ahlswede, J. Weis, F. Dahlem, J. G. S. Lok, and K. von Klitzing for stimulating discussions.

References

1. K. von Klitzing, G. Dorda, and M. Pepper, *Phys. Rev. Lett.* 45, 494 (1980).
2. H. Bachmair, E. O. Göbel, G. Hein, J. Melcher, B. Schumacher, J. Schurr, L. Schweitzer, and P. Warnecke, *Physica E* 20, 14 (2003).
3. E. Ahlswede, P. Weitz, J. Weis, K. von Klitzing, and K. Eberl, *Physica B* 298, 562 (2001).
4. A. Siddiki and R. R. Gerhardt, *Phys. Rev. B* 70, 195335 (2004).
5. A. Siddiki and R. R. Gerhardt, *Int. J. Mod. Phys. B* 18, 3541 (2004).
6. B. Kramer, S. Kettmann, and T. Ohtsuki, *Physica E* 20, 172 (2003).
7. M. Büttiker, *Phys. Rev. B* 38, 9375 (1988).
8. D. B. Chklovskii, B. I. Shklovskii, and L. I. Glazman, *Phys. Rev. B* 46, 4026 (1992).
9. E. Ahlswede, J. Weis, K. von Klitzing, and K. Eberl, *Physica E* 12, 165 (2002).
10. P. Weitz, E. Ahlswede, J. Weis, K. v. Klitzing, and K. Eberl, *Physica E* 6, 247 (2000).
11. P. Weitz, E. Ahlswede, J. Weis, K. v. Klitzing, and K. Eberl, *Appl. Surf. Sci.* 157, 349 (2000).
12. D. Pfannkuche and J. Hajdu, *Phys. Rev. B* 46, 7032 (1992).
13. J. H. Oh and R. R. Gerhardt, *Phys. Rev. B* 56, 13519 (1997).
14. K. Güven and R. R. Gerhardt, *Phys. Rev. B* 67, 115327 (2003).
15. R. R. Gerhardt, *Z. Physik B* 21, 285 (1975).
16. T. Ando and Y. Uemura, *J. Phys. Soc. Japan* 36, 959 (1974).
17. T. Ando, A. B. Fowler, and F. Stern, *Rev. Mod. Phys.* 54, 437 (1982).
18. D. B. Chklovskii, K. A. Matveev, and B. I. Shklovskii, *Phys. Rev. B* 47, 12605 (1993).
19. K. Lier and R. R. Gerhardt, *Phys. Rev. B* 50, 7757 (1994).
20. T. Suzuki and T. Ando, *Physica B* 227, 46 (1996).
21. T. Suzuki and T. Ando, *Physica B* 249-251, 415 (1998). Further references therein.